

SYLVIUS: A multimodal and multidisciplinary platform for epilepsy surgery

Alfredo Higuera-Esteban^{1,2}, Ignacio Delgado-Martínez¹, Laura Serrano³, Alessandro Principe⁴, Carmen Pérez Enriquez⁴, Miguel A. González Ballester^{2,5}, Rodrigo Rocamora⁴, Gerardo Conesa³, Luis Serra¹

¹Galgo Medical SL, Neurosurgery Dept, Barcelona, Spain

²Universitat Pompeu Fabra, BCN Medtech, Dept. of Information and Communication Technologies, Barcelona, Spain

³IMIM-Hospital del Mar, Neurosurgery, Barcelona, Spain

⁴IMIM-Hospital del Mar, Epilepsy Unit, Barcelona, Spain

⁵ICREA, Barcelona, Spain

ABSTRACT

Background and objective: We present SYLVIUS, a software platform intended to facilitate and improve the complex workflow required to diagnose and surgically treat drug-resistant epilepsies. In complex epilepsies, additional invasive information from exploration with stereoencephalography (SEEG) with deep electrodes may be needed, for which the input from different diagnostic methods and clinicians from several specialties is required to ensure diagnostic efficacy and surgical safety. We aim to provide a software platform with optimal data flow among the different stages of epilepsy surgery to provide smooth and integrated decision making.

Methods: The SYLVIUS platform provides a clinical workflow designed to ensure seamless and safe patient data sharing across specialties. It integrates tools for stereo visualization, data registration, transfer of electrode plans referred to distinct datasets, automated postoperative contact segmentation, and novel DWI tractography analysis. Nineteen cases were retrospectively evaluated to track modifications from an initial plan to obtain a final surgical plan, using SYLVIUS.

Results: The software was used to modify trajectories in all 19 consulted cases, which were then imported into the robotic system for the surgical intervention. When available, SYLVIUS provided extra multimodal information, which resulted in a greater number of trajectory modifications.

Conclusions: The architecture presented in this paper streamlines epilepsy surgery allowing clinicians to have a digital clinical tool that allows recording of the different stages of the procedure, in a common multimodal 2D/3D setting for participation of different clinicians in defining and validating surgical plans for SEEG cases.

KEYWORDS

Epilepsy surgery – Stereotactic electroencephalography (SEEG) – Diffusion-weighted imaging (DWI) – Surgical workflow – Multimodal - Multidisciplinary

HIGHLIGHTS

- Efficient transfer of information among epileptologists and neurosurgeons.
- Scenograph-based processing pipeline to drive registration of multiple datasets.
- Graphics processing unit (GPU) based detection of vessels for a planned trajectory.
- Specialized DWI tractography tools for SEEG.
- Semi-automatic electrode segmentation tool.

1. INTRODUCTION

1.1. Epilepsy treatment

Around one third of epilepsy patients do not respond to anti-epileptic drugs [1][2] and are potential candidates for epilepsy surgery, a procedure which consists on the removal or disconnection of the epileptogenic zone (EZ). Defining the EZ is a complex issue [3] but some definitions are: “the site of the beginning and of primary organization of the epileptic seizures” [4,5] or “the minimum amount of cortex that must be resected (inactivated or completely disconnected) to produce seizure freedom”[6].

Thanks to intraoperative neurophysiological monitoring and careful presurgical planning it is possible to safely operate in a variety of areas inside the brain, although sometimes surgery must be discarded (e.g.: when the EZ cannot be located). Epileptologists usually study the semiology and may employ a variety of non-invasive techniques to locate the EZ like electroencephalography (EEG), magnetic resonance imaging (MRI), positron emission tomography (PET), or single-photon emission computed tomography (SPECT)[7].

When non-invasive techniques fail to locate the EZ, invasive diagnostic techniques such as stereotactic electroencephalography (SEEG) can be used. SEEG was developed in the second half of the last century [8] and has since then made great progress alongside 3D multimodal imaging and the use of new surgical devices, in particular robots. Despite these advances, the core methodology remains unaltered, consisting in the stereotactic placement of a number of intracerebral depth electrodes for several days (Gonzalez-Martinez et al. reported 7 days on average [9]), yielding precise electrical recordings of brain activity both during and between seizures.

It is usual for the SEEG planning to start with an initial plan proposed by the epileptologist based on an EZ localization hypothesis to prove or discard the presence of the EZ in several possible locations. This plan is then discussed with the neurosurgeons who can use different systems (frame-based, frameless, and robotic[10]) for the implantation. The next step is usually to introduce the initial epileptology plan into a surgical planning software -many times provided by the stereotactic neurosurgical hardware manufacturer- and refine it to mitigate surgical risks, which may require new imaging modalities. Despite the increasing sophistication of these tools, the planning process still involves manual scrolling through

the image planes to find avascular trajectories, which has been described in the literature as an error-prone, inefficient, and time-consuming process [11].

If the EZ is identified, the final step is for the epileptologist to delineate the area of the brain to be removed and for the neurosurgeons to use the most suitable surgical approach to perform the intervention. This could be a craniotomy followed by a resection, laser ablation, or radiofrequency thermocoagulation [12]. Again, precise communication between epileptologists and neurosurgeons is crucial.

Being multidisciplinary, epilepsy surgery may present strong multimodal requirements. Adding to the previously mentioned datasets, modalities like double-contrast Gadolinium MRI (T1-Gd), Angio-CT with bolus injection or digital subtraction angiography (DSA) among others may be used to avoid vasculature, computer tomography (CT) may be used during the intervention for registration with the frame/robot and after electrode implantation for validation, and diffusion-weighted imaging (DWI) and functional magnetic resonance imaging (fMRI) can be of use to locate functional areas to protect and to study EZ connectivity. Neuroscientists sometimes play a support role in processing DWI using tools such as MITK-DI [13], Startrack [14], or MRtrix [15], voxel-based morphometry (VBM) [16], analyzing fMRI [17], running source localization algorithms [18] or performing segmentation tasks [19], providing even more datasets.

The presented work describes a new system aiming to provide a patient-centered application structure that allows for storing and sharing different stages of SEEG and epilepsy surgery. It describes both a workflow, as well as several generic and specific tools.

1.2. Related work

The Ospedale Niguarda group [20,21] has extensive experience in the surgical treatment of epilepsy and the use and development of several software tools for it. Their workflow introduced the use of DSA for the multimodal evaluation of SEEG implantation [22], where DSA constitutes the reference space to which all datasets are registered. The group presented a 3D Slicer module to automatically define SEEG trajectories given a target point and possible entry points [23,24]. In [25] a tool is presented in which, for each electrode, a maximum intensity projection (MIP) image is obtained by projecting a portion of one centimeter of the vessel volume on a plane perpendicular to the electrode trajectory. Yet another 3D Slicer module was presented in [26] dedicated to assisting the clinical team in the post-implant stage. 3D Slicer input is untagged, and the tools are usually configured selecting datasets by name from drop-down lists.

Another relevant platform is EpiNav [27], which has a dedicated user interface specially designed for epilepsy, and it has been used as a clinical decision support tool [28]. It allows for multimodal image registration [29], 3D mesh model generation and visualization, and manual and automated electrode planning among other features. Images are imported into the case through drag and drop. Data import is again untagged, and tools require the user to identify the input datasets by name from all the imported ones. In [30] a pipeline for the creation of multimodal cases is presented which is an attempt to provide a comprehensive workflow. It describes a fixed image integration scheme, where all datasets are registered to a T1-weighted image. EpiNav also provides a risk profile visualization along the trajectory designed to easily inform the surgeon of the vicinity of risks along a given trajectory [31]. EpiNav can also import Freesurfer segmentations.

IBIS [32,33] is a neuronavigation system that incorporates an automatic planner for SEEG with the novelty that it attempts to maximize intracranial EEG recording from the volume of interest and its surroundings.

It is a system with advanced Augmented Reality (AR) and registration capabilities. It organizes datasets in a hierarchical structure, where each node contains a transform (i.e.: a mathematical operation that allows modifying the medical dataset location in 3D space), and it is concatenated with the transform of its parent nodes, which prevents image resampling upon registration. In [34] they use tubes -instead of lines- to represent electrode trajectories, a feature that can also be found in commercial systems to define a security zone surrounding the electrode. To the best of our knowledge, this software can be used for SEEG interventions, but no concept of workflow is built into the platform.

A procedure that shares some similarities with SEEG is Deep Brain Stimulation (DBS), where software solutions like Cirerone [35] and CranialVault [36] have been developed to address the issue of workflow and data transfer among the various stages. In [37] a tool is presented for the optimization of DBS electrodes based on geometric constraints. The tool focuses on the risk computation of insertion points (or entry points) for a given target point. A visualization of the risks associated with each entry point is presented, designed to facilitate decision making. Despite similarities with SEEG, in DBS the target point is fixed (is the point to be stimulated) whereas in SEEG both the entry and the target point can be moved, and risk visualization projected on the cortex does not seem suitable for displaying the entire set of possible trajectories.

AR and VR have been proposed to aid both at the pre-operative and intra-operative [38] stages of the planning and insertion of rectilinear trajectories inside the brain. The Dextroscope [39] is a VR environment that provides a 3D representation of the patient data based on multimodal volume rendering. The user can manipulate the 3D rendered image with two handheld controllers, allowing for intuitive exploration of the surgical field as well as three-dimensional planning of rectilinear trajectories. In [40] an AR planning system was presented which only presents blood vessels and critical structures in the vicinity of the planned trajectory allowing the user to concentrate only on the relevant structures. Our work aims to integrate this functionality in those places where it may be required in the context of epilepsy surgery planning.

In conclusion, epilepsy surgery is a complex procedure with strong multimodality requirements, but there are also multidisciplinary concerns (i.e.: fluid communication across the different specialties involved in the procedure), which have to our knowledge not yet been fully addressed. Furthermore, we also aim to simplify the currently available user interfaces and interactions required.

1.3. Design principles and main technical contributions

SYLVIUS is a platform that integrates different tools along the epilepsy surgery workflow, and which could be used in a clinical environment. Its workflow is defined by the different SEEG electrodes stages and the final resection: starting from a preliminary plan, the initial surgical plan, a reviewed plan, the executed surgical plan (which can be modified in the operating room), the final postoperative segmented SEEG electrodes and the resection plan. Although the workflow is particularly designed to the way epilepsy surgery is performed in our institution, we believe its general principles can be applied to different implementations of the procedure by modifying small parts of the application. To the best of our knowledge, no other tool has been presented which can represent so many steps of the epilepsy surgery workflow.

For the implementation, we have tried to follow these design principles:

- The clinical user must be able to transfer/compare information from different workflow steps without having exposure to matrices or other mathematical constructs.
- Annotate the data upon import and use that information to automatically configure inputs and rendering parameters. Tools become active only if all required inputs are present and co-registered.
- Avoid image degradation upon registration. The negative effects of image interpolation and resampling [41] can be especially relevant in this procedure due to the number of images involved and the multiple registrations required to merge them.
- Allow a flexible order in which the DICOM images are loaded and registered to each other. The registration scheme should not be fixed.

In the graphical user interface (GUI) domain, a draggable tree diagram with nodes representing the different datasets has been developed to drive registrations, substituting drop-down lists, and giving an idea of the actual registration state.

SYLVIUS also includes several innovations in processing and visualization tools, such as a novel tool to detect DSA vessels inside the security zone, the possibility to filter DWI tractography directly with SEEG electrodes, and the ability to display electrophysiological data directly over the contacts that measure it.

2. DESCRIPTION OF THE SYSTEM

SYLVIUS is implemented in the C++ programming language and uses a Python wrapper over CMake for project configuration. It uses the wxWidgets library for the Graphical User Interface. VTK, ITK, and MITK are used for visualization, registration, and processing. The overall architecture is plugin based and the structure of the code imposes a clear separation between processing and interaction code. SYLVIUS is only distributed for Windows although its components and its build chain are cross-platform.

When used in a zSpace 300 system (zSpace, Inc., USA), SYLVIUS offers 3D interaction and stereo visualization for working with complex 3D structures (like vessels or white matter tracts, which have geometries that may be hard to visualize in 2D planes and anticipate its shape, unlike, say, a round-shaped tumor). This hardware (depicted in Figure 1) is composed of a computer, a stereo screen that emits circularly polarized light, and an integrated infrared tracking system which allows for pose retrieval (6 degrees of freedom) of polarized glasses and a 3D stylus.

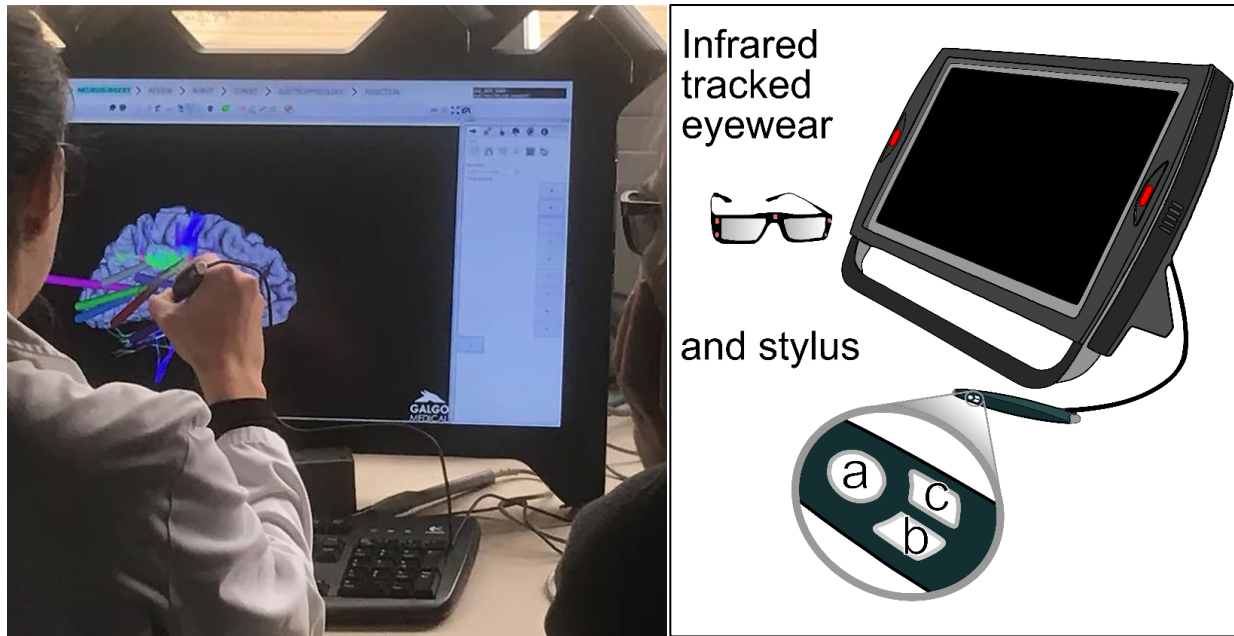


Figure 1 zSpace systems consisting of a stereo screen with integrated infrared tracking, tracked eyewear, and a tracked 3D stylus with three buttons.

The zSpace glasses movement events are directly connected to a custom subclass of a VTK camera, which renders the scene using two non-symmetric frustums, one for each eye. This technique adds parallax depth cues to the stereo visualization which is intended to reduce the cognitive load associated with the understanding of complex 3D shapes (such as vessels and tractography). Head-tracking is used to provide yet another functionality: the near clipping plane of the aforementioned frustums moves with the tracked glasses allowing the user to clip the scene and examine the internals of a dataset just by moving the head closer to the screen.

2.1. Tools common to all disciplines

2.1.1. Case Management and Graphical User Interface

Upon start-up, the user can either create a new study or open a previous one. Cases are saved to disk using an internally developed data structure formed by a combination of XML and VTK file formats. A search box allows users to filter cases by patient name. When a new case is created, the software presents itself with most tools disabled (Figure 2) which get activated once their required datasets are imported or become registered.

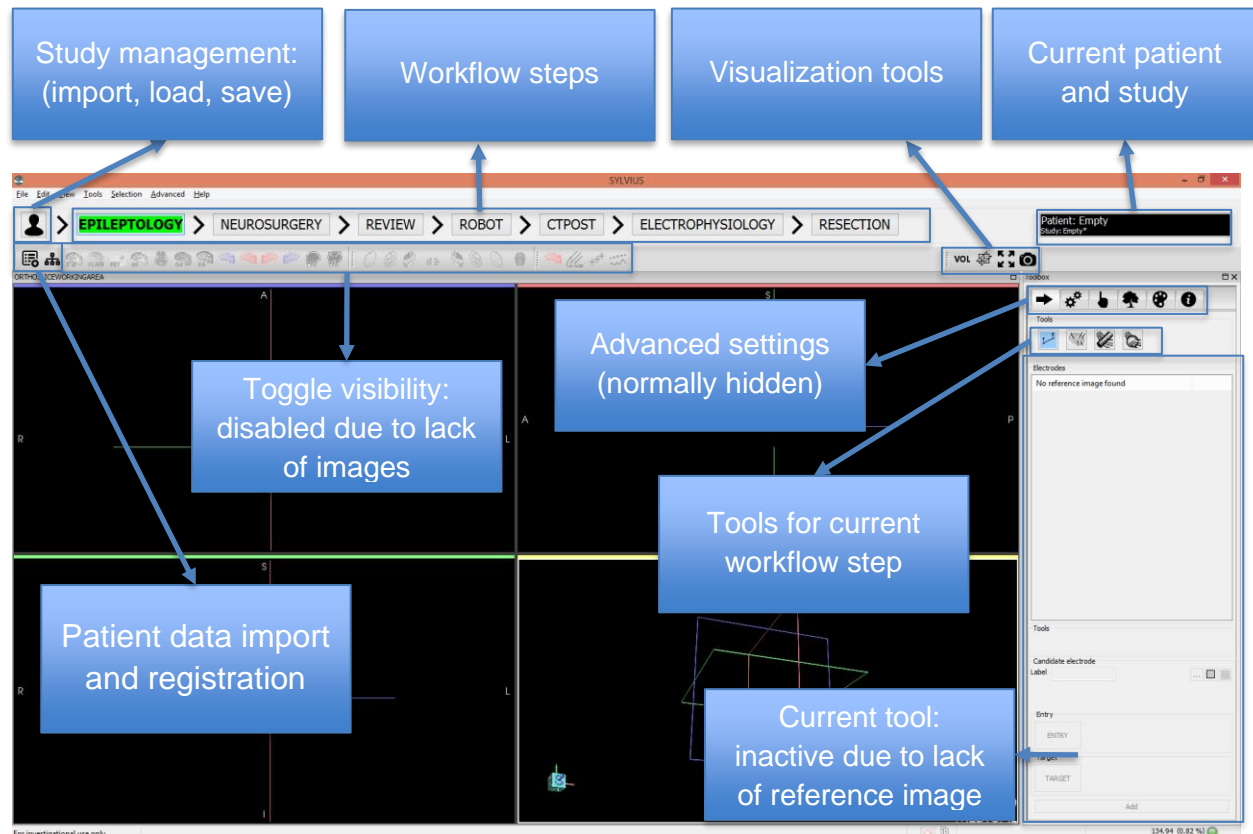


Figure 2 General description of SYLVIVUS graphical interface

2.1.2. Data import

The data import button displays a pop-up window as depicted in Figure 3. When a specific modality button is pressed, and a file/folder is selected for import, the volume is loaded annotated as that modality, rendering parameters associated with that modality are applied, relevant processing tools are enabled, the visualization toolbar is updated and the image is marked as present in the import window. This interaction follows our design principle of tagging data upon import.

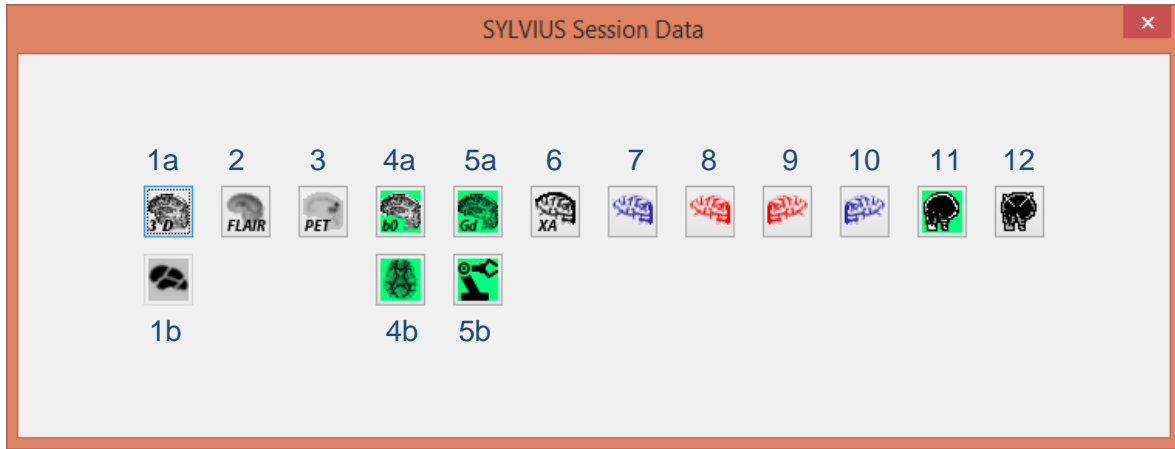


Figure 3 Pop-up window for centralized data loading. The datasets already loaded are marked with a green background. (1a) **T1-weighted**, (1b) **Freesurfer**, (2) **FLAIR**, (3) **PET**, (4a) **b0** from diffusion tensor imaging, (4b) **Tractography** (5a) Double-contrast gadolinium magnetic resonance **T1-Gd**, (5b) Robot plan, (6-10) X-ray angiographies, one without contrast and four with contrast -left and right, arteriograms and the venograms- **XA**, (11) Preoperative Computerized Tomography **CTpre**, (12) Postoperative Computerized tomography **CTPost**.

Paired datasets, which rely on the presence of other reference data modalities, are presented below their required ones (1b, 4b, and 5b in Figure 3) and are disabled if their reference data is not yet imported. For example, tractography (which is generated externally and imported in TrackVis [42] format) requires the presence of the b0 volume which will be later required for registration.

2.1.3. Registration GUI and Restrictive Scene Graph

SYLVIUS implements a hierarchical data structure similar to [32]: a scene graph. Registration data is stored in relative transform nodes, which modify the pose of their children. This approach avoids unnecessary image degradation [41] upon registration. SYLVIUS uses procedures contained in the MITK framework [43] for registration.

The platform relies on user expertise to choose the pairs of images to register, providing a flexible registration scheme. As in [31], we consider brain shift to be negligible. To prevent mirroring, relative transform nodes are only allowed to contain proper rigid transforms (i.e., matrix determinant must be equal to 1). For dependent datasets (e.g., Freesurfer [19]) the import procedure creates the relative transform node and no further registration is required nor allowed for them.

SYLVIUS provides a simplified scene graph window to manage registrations graphically. It displays only the most relevant datasets, represented with the same icons as the import window and visualization toolbar. A registration procedure is launched by dragging any non-previously registered image icon and dropping it on top of any other volume, as depicted in Figure 4. If the registration is validated the view becomes updated and the dragged image and all its children become affected by the computed transformation.

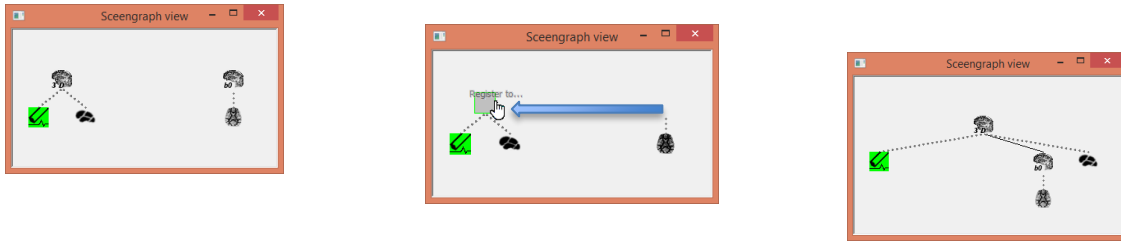


Figure 4 Registration GUI. Left: the initial state of the study containing T1 (depicted as 3D), its Freesurfer segmentation and an epileptology electrode plan referenced to it, and an unregistered b0 volume with its dependent tractography. Middle: Launching registration with T1 as fixed image and b0 as moving image by dragging b0 on top T1. Right: after registration session shows all present datasets are registered. Dotted lines represent fixed relationships, and a solid line depicts a relative transform node generated by a registration.

When a dataset is imported, it starts as being disconnected from the rest. To assess that all datasets are registered the user needs only to check that there is a unique tree, as the one depicted in Figure 5.

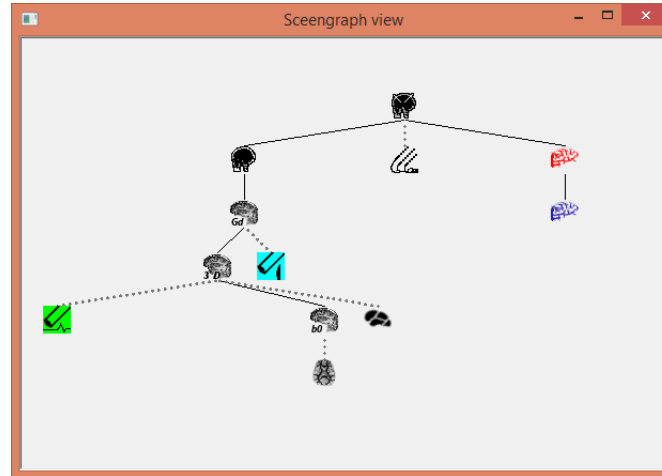


Figure 5 Fully registered case, containing several volumes (CTpost, CTpre, MR2c, T1 with Freesurfer, b0 with tractography and two XA) and 3 electrode sets (epileptology, surgery, and the CTpost segmented one).

2.2. SYLVIOUS Workflow

The workflow is defined by the following steps:

2.2.1. Epileptology

The first step in the workflow is taken by epileptologists to define a preliminary SEEG plan. Importing a T1-weighted image is the only prerequisite to adding electrode trajectories, which are stored as children of the T1-weighted image in the scene graph. At this stage, it is common to import a Freesurfer segmentation or to import a FLAIR and a PET.

A mouse trajectory planning tool (Figure 6) provides a multi-render window with either an orthogonal view or a “probe’s eye view” -as described in [25]-, both of them with an accompanying 3D view. To aid in multidisciplinary, the epileptologist can leave comments to the neurosurgeon on a per electrode basis.

It is also possible to add, modify and delete trajectories in a single 3D stereo window using the zSpace 3D stylus.

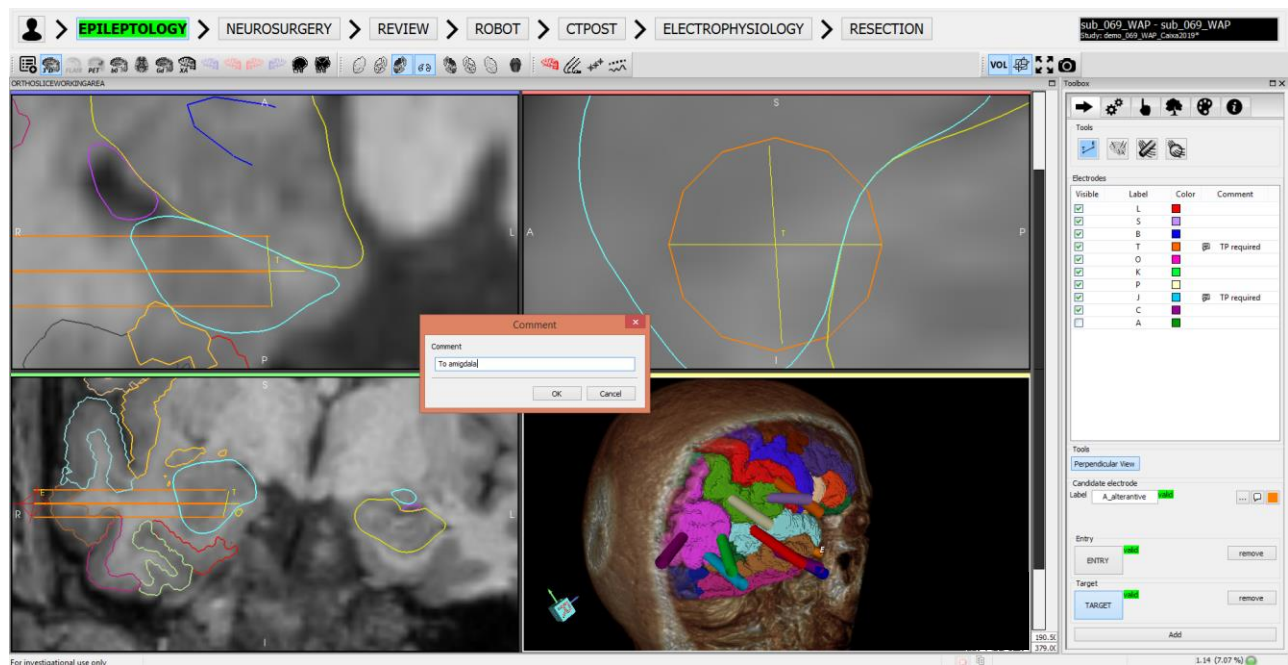


Figure 6 Epileptology step: mouse trajectory planning in “probe’s eye” view (aligned with the trajectory) plus a 3D view of volume-rendered MRT1 and meshes from Freesurfer segmentation. Adding a comment for trajectory inside the amygdala.

2.2.2. Neurosurgery

This step is intended for the neurosurgeon to define the first version of the surgical plan based on the previous electrode set. An MR2c image is required to place electrodes. Up to four XA images can be imported to provide greater insight into the vessel structure of the patient.

A “Clone” button allows to precisely transfer the epileptology plan to neurosurgeons, even though they are referred to different coordinate systems (i.e., reference images). The button is enabled when the T1-weighted and MR2c images get co-registered. When clicked, it shows a list of the electrodes from the *epileptology electrode set*, which can be selected to copy that trajectory in the neurosurgery working area by transparently applying all necessary transformations defined in the scene graph (from T1-weighted space to the MR2c space). Upon cloning, comments show up in a pop-up window.

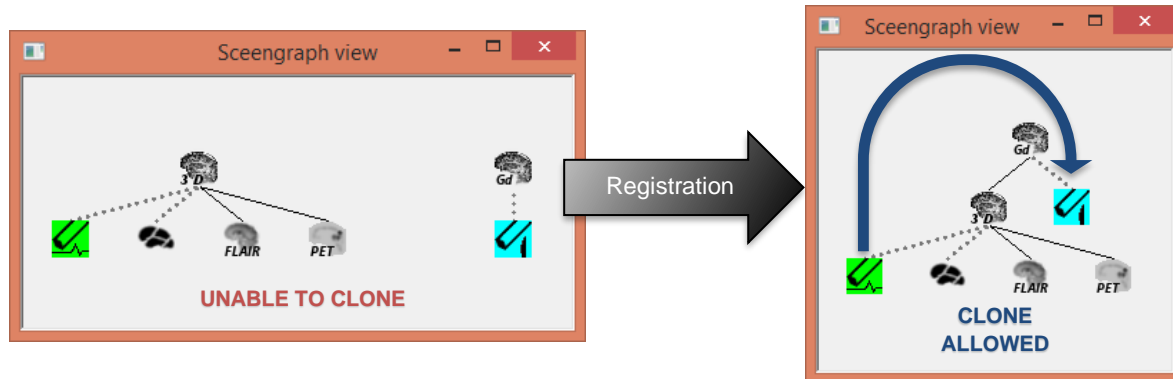


Figure 7 A session with several images loaded before (left) and after (right) registration of the T1 and the MR2c images. Once they are registered the electrodes can be cloned from the Epileptology electrode set (green) into the Neurosurgery electrode set (blue).

Another specific tool of this step is a novel tool to detect collisions of the security zones of the electrodes with vessels briefly described in [44]. This tool is similar to the MIP tool presented by [25] but projects the vessels along the full trajectory. Instead of projecting the maximum intensities, depth is recovered from the z-buffer of the rendering pipeline, which is stored and used for two purposes. When the user clicks on a vessel in the 2D projected image it is used to un-project the 3D point, centering the tri-planar axes on that vessel. Second, depth is mapped to brightness in the projected view, where brighter means closer to entry (Figure 8).

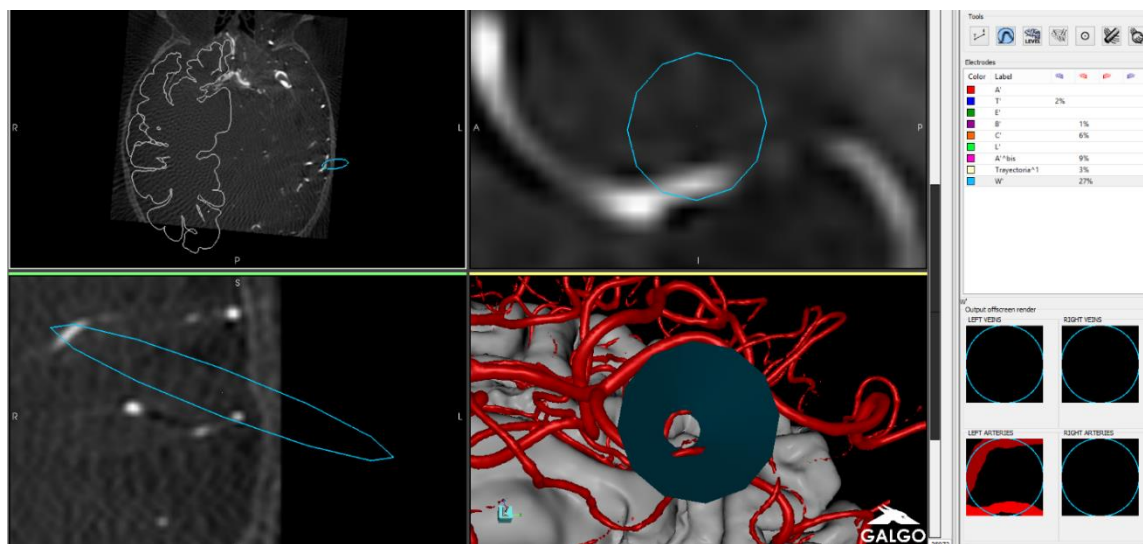


Figure 8 Neurosurgery step. Tool similar to MIP to early detect vessels from up to four XA studies inside the security zone of the planned electrode. For the selected electrode (W') tool indicates 27% of pixels inside the security zone as collisions, which correspond to two distinct vessels at a different depth.

A toolbar button renders the *epileptology* electrode set (in green wireframe) for a fast visual comparison of the two versions of the plan (Figure 9).

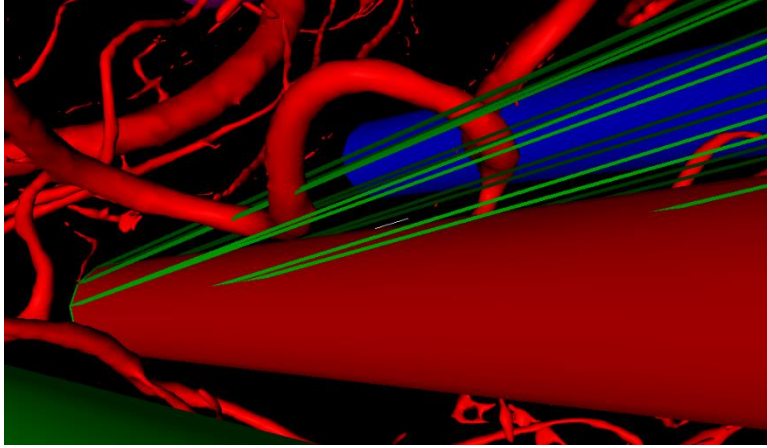


Figure 9 Neurosurgery step: An electrode trajectory (solid color) compared with the one defined in the epileptology step (green wireframe). Its entry point has been modified to avoid hitting a vessel detected in the XA image.

2.2.3. Review

This step is intended to be used as a consolidation tool in a multidisciplinary meeting between epileptologists and surgeons. The participants can clone one by one each electrode from the neurosurgery electrode set and check if the modifications performed by the neurosurgeon still measure the desired areas of interest for the epileptologist.

This tab also contains tools to export the electrode set to the intraoperative system in a text file (for our intraoperative prototype), in DICOM format, or navigating to the entry and target point of each electrode in the tri-planar view.

2.2.4. Robot

During the electrode implantation, the plan present in the intraoperative system (currently ROSA) can be loaded back into SYLVIUS to keep it synchronized with intraoperative modifications. This also provides enhanced views including images that may not be present in the intraoperative system, as well as advanced tools from SYLVIUS. Furthermore, this also allows us to later analyze intraoperative modifications of the reviewed plan and their causes.

2.2.5. CTpost

Once the SEEG electrodes have been implanted, their final position can be obtained from a postoperative CT and managed in the CTpost step. This segmentation obtains the location of each contact (5-18 contacts per electrode). Manually segmenting these contacts is a tedious task, and tools like DEETO [45], Epitools [46], and SEEG Assistant [26] allow for automatic identification of contacts. Our approach to contact segmentation is described in [47], which only requires the CTpost image.

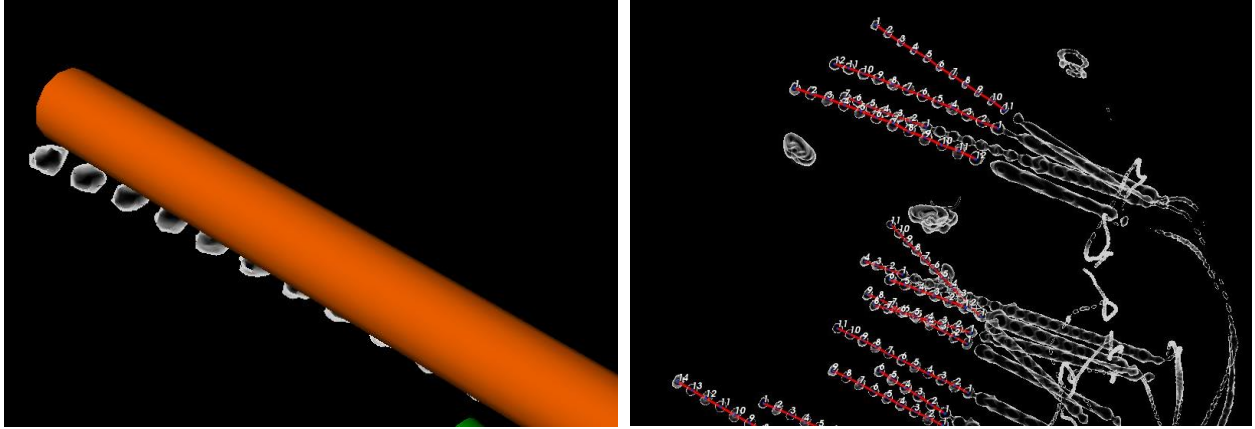


Figure 10 Left: upon registration, the user can compare the surgical plan referred to MR2c with the real outcome (using our segmentation method on the postoperative CT). Right: contact segmentation tool.

2.2.6. DWI tractography

SYLVIUS itself does not process DWI but it can import a b0 and a whole-brain tractography computed with Startrack [14], Dextroscope[39] in TrackVis [42] format. It is possible to perform freehand 3D stereo tract filtering with a spherical region of interest (ROI) which is positioned with the 3D stylus (Figure 11). It is also possible to perform electrode-based tract filtering. The simple mode allows the clinician to filter the tracts that traverse the security zone of one or multiple electrodes simultaneously (AND operation), as depicted in Figure 11.

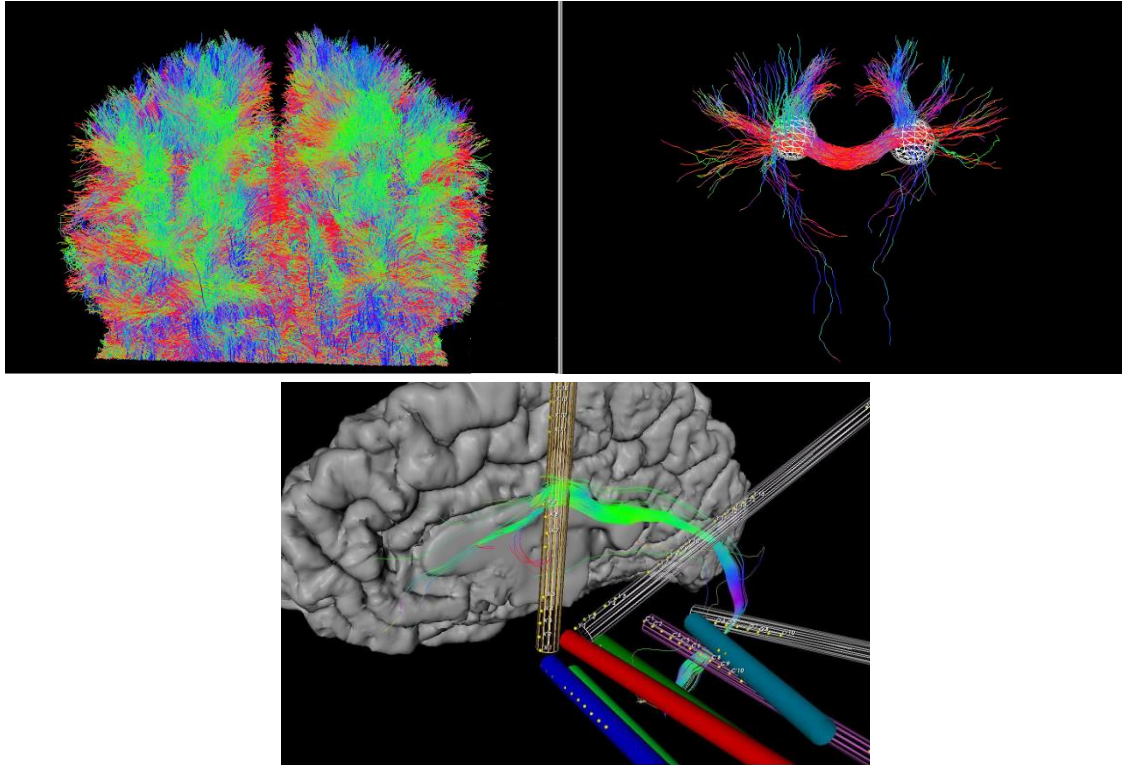


Figure 11 Top: a whole-brain tractography before and after being filtered with two spherical ROI with the AND operation. Bottom: A filtered DWI tractography, displaying only the tracts which traverse the four selected electrodes security zones (in wireframe). The final contact position segmented from CTpost is displayed (yellow spheres).

SYLVIUS can perform a more fine-grained computation to attempt to shed some light on the relation between electrical data measured (SEEG contacts) and the tissue involved in its transmission (tractography), which we have called the SEEG-electrome[48]. This requires a b_0 and its corresponding tractography analysis to be registered with the CTpost volume, from which the contact positions are obtained. It then first creates a set of spherical ROIs, either centered on each segmented contact (for unipolar measurements) or placed in the gap between two contacts (for bipolar measurements). Then, it computes all the tracts which traverse at least two contact ROIs at the same time.

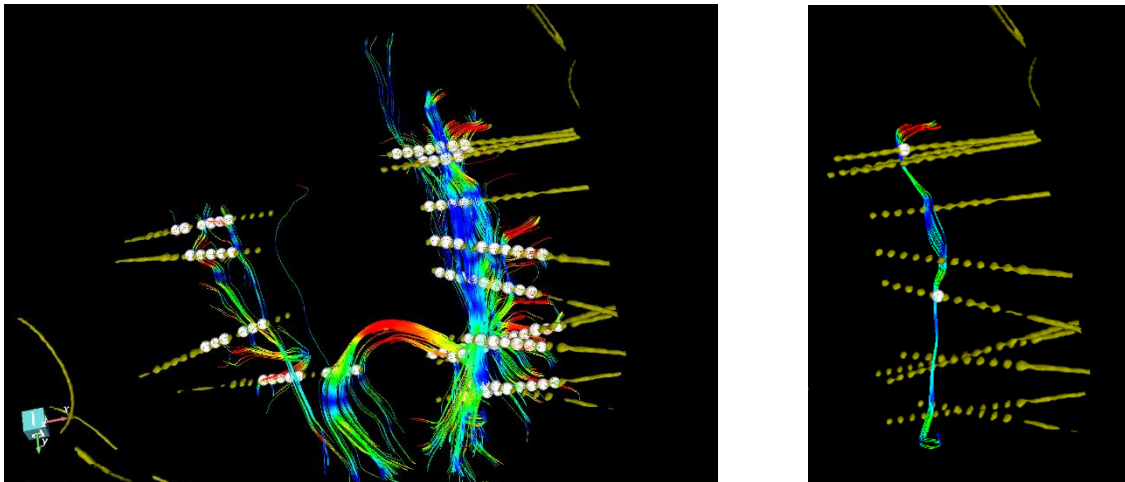


Figure 12 SEEG-Electrome computation of a patient with bilateral implantation of SEEG electrodes. Left: aggregated result of the computation. Right: single result from a pair of bipolar spherical ROIs (from SEEG) and the tracts which connect them anatomically (according to the DWI tractography).

2.2.7. Electrophysiology

This step provides tools to load and play raw SEEG electrical signals in 3D+t. Data are imported in the European Data Format (EDF) file format, where each signal must have the same name as each contact (i.e., electrode label plus a number). Voltages are normalized and mapped to a color scale used to shade a cylinder of the size of real contact.

Although the presented tool is designed to visualize the raw SEEG readings, it can be used to display the results of electrical data analysis such as correlation analysis or epileptogenicity as in [46].

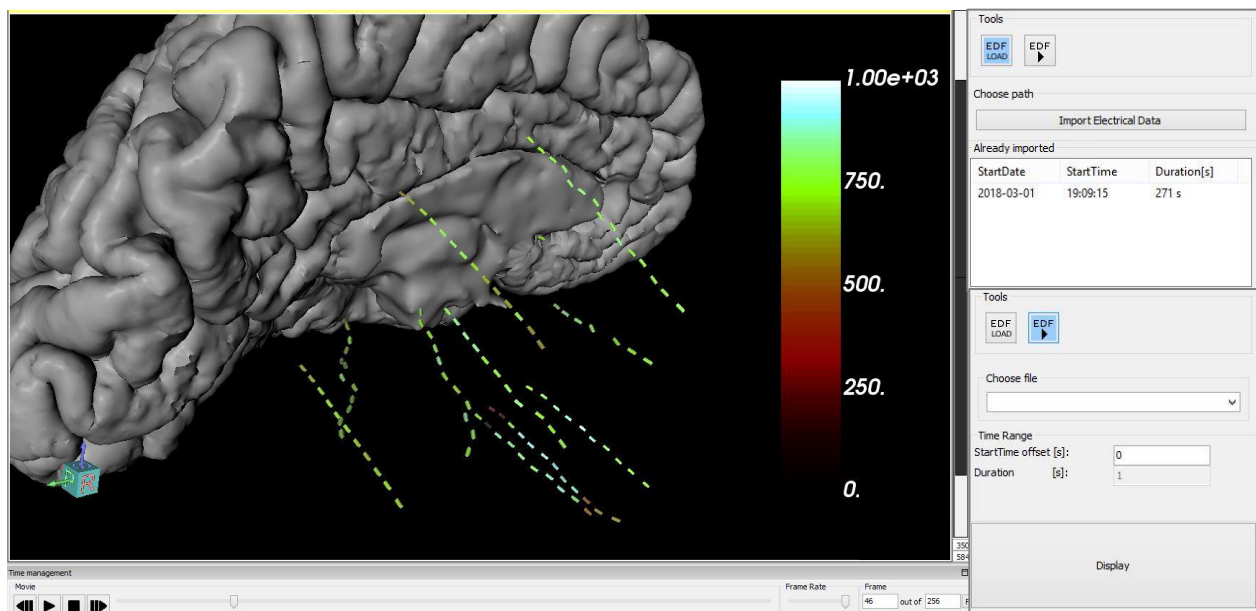


Figure 13 Left: A frame of a 3D+t representation of the electrical signals mapped onto the contact it was measured from. Top right: EDF import tool. Bottom right: EDF play tool.

2.2.8. Resection

In this last step of the workflow, the epileptologist – based on data collected so far— proposes a resection area of the brain that is revised with the neurosurgeon (Figure 14). This step of SYLVIUS allows for a segmented portion of the cortex to be exported in DICOM to the neuronavigation system, in our case the Stealth Station (Medtronic).

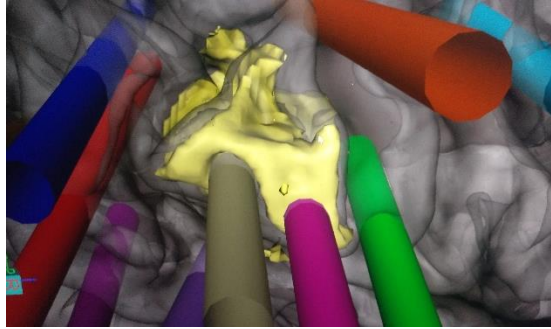


Figure 14 Area of the cortex marked for resection.

The development of SYLVIUS has accompanied the implantation procedures in Hospital del Mar, Barcelona, Spain (member of EpiCARE, a European Reference Network for rare and complex epilepsies) from 2016 to the present day (58 cases), in progressively higher degrees of involvement. Informed consent was obtained from all patients or their guardians for the data to be used in scientific research and publication (Ethical Committee on clinical investigations Parc de Salut MAR, 2014/5940/I). It has been used to visualize patient data in pre, intra, and postimplantation stages of SEEG, both in 2D and in stereo 3D, and has allowed for the planning and postoperative analysis of SEEG electrodes. As the platform is designed to cover multiple stages of the epilepsy workflow distinct partial results will be presented, all of them integrated by the described architecture.

To evaluate its use as a preimplantation planning tool for SEEG, 19 cases (8 with T1-Gd, and 11 with T1-Gd and DSA) were evaluated. For each patient, modifications from the draft plan following the design provided by the epileptologists to the reviewed surgical plan were analyzed, as well as the reasons given by the neurosurgeons for each change. Reviewed plans were transferred to the ROSA system before the implantation, where the neurosurgeon gave the final approval.

3. RESULTS

No complications were reported after the interventions. From the 217 trajectories analyzed within SYLVIUS, 7 were erased, 78 remained unchanged, and the rest had their entry (53), target (10), or both (69) modified. Percentages can be seen in Figure 15, both individualized and grouped by the presence or not of DSA. The reasons given for the modifications -aggregated by the presence or not of DSA- are shown in Figure 16.

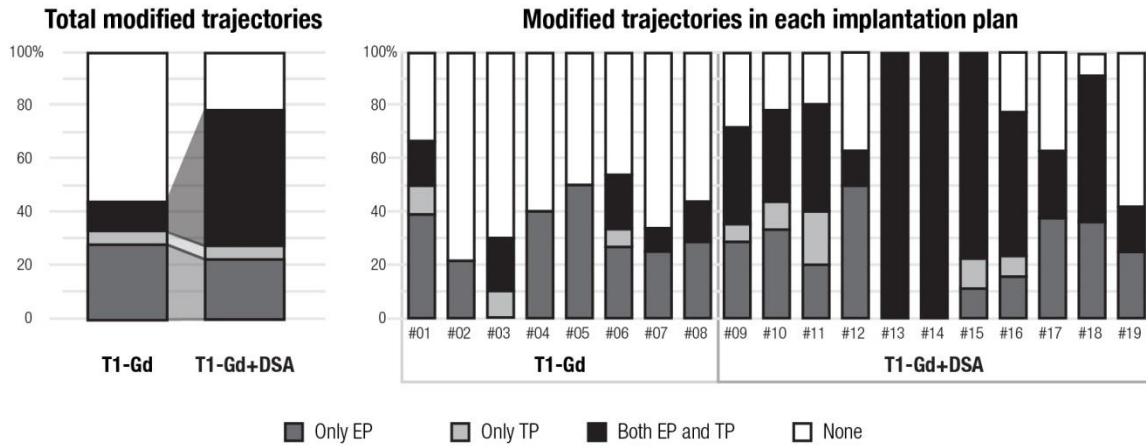


Figure 15 Modified trajectories within SYLVIUS for 19 retrospective cases.

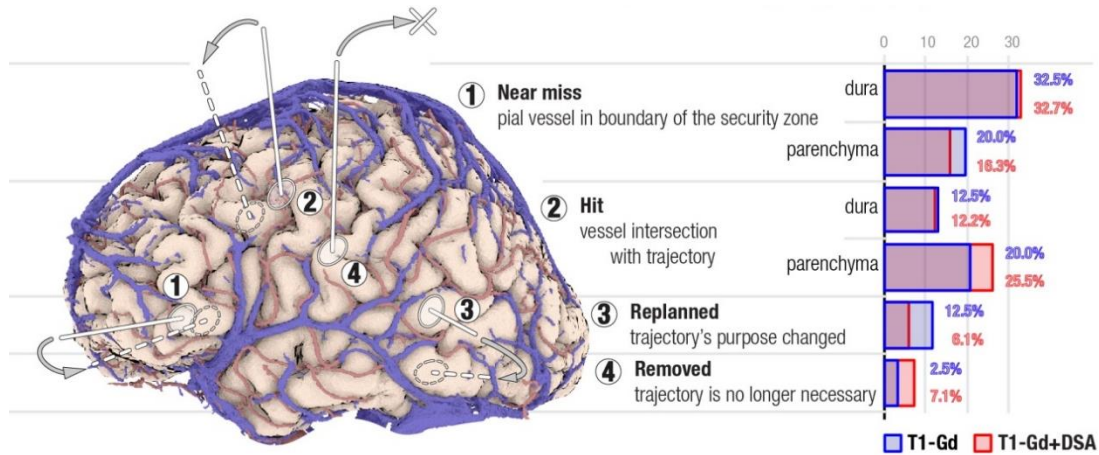


Figure 16 Reasons given by the neurosurgeons for the modification of SEEG trajectories by group.

Also in the preoperative stage, the vessel collision detection tool was compared to 2D inspection by a trained neurosurgeon[44], correctly detecting 79.5% of them in under 4 seconds. The only cause for false negatives was low-intensity vessels (below 1500 HU) removed by the threshold segmentation.

In the postimplantation stage, our electrode segmentation tool [47] was used to segment the final position of SEEG electrodes on 24 postoperative CT scans from 18 patients. From a total of 327 electrodes (DIXI Medical) containing 3663 individual contacts, SYLVIUS was able to correctly identify up to 274 with at least 4 contacts, and correctly localize 2422 contacts (66%) in approximately half a minute per case. A comparison of the results of this computation with a manual segmentation can be seen in Figure 17.

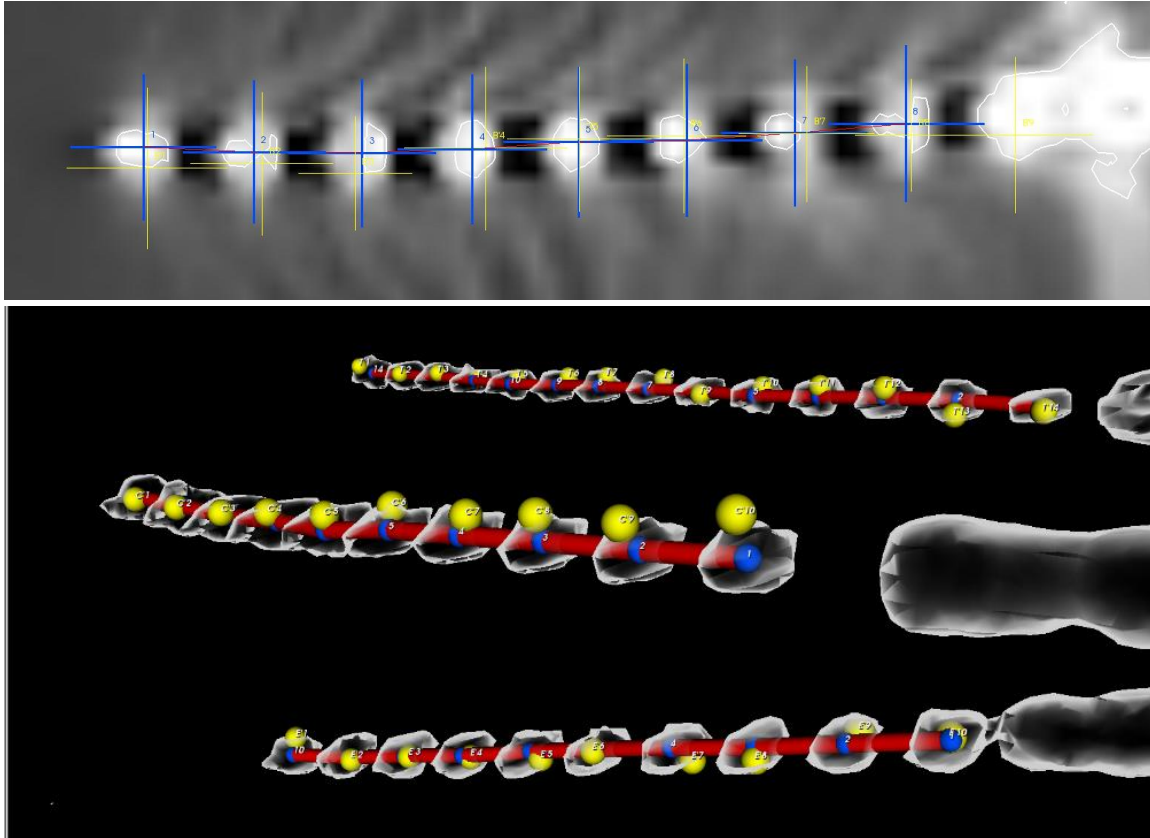


Figure 17 Comparison of the automatic (blue crosses and spheres) and manual (yellow crosses spheres) contact segmentation of SEEG electrodes from a postoperative CT scan.

The SEEG-electrome computation was analyzed [48] in a real clinical case with 163 contacts from 15 electrodes -defining a total of 148 electrical ROIs- and a whole-brain tractography, revealing 147 connections (Figure 12) from over 10.000 ($\binom{148}{2}$) possible pairs. The detected bipolar ROIs sometimes connected ROIs located on the same electrode and sometimes connected distant areas of the brain (e.g.: frontal to occipital) from two different electrodes.

4. DISCUSSION AND FUTURE WORK

One of our guiding principles has been to create tools in which the user requirements are expressed in terms of data availability and validated registrations. Examples of this design are the tractography filtering tools, the functionality to compare and transfer trajectories, or the DSA vessel collision detection tool. The users have been presented with tools that attempt to simplify case construction -such as the data import and the registration widgets- which allow for graphical registration of multimodal datasets. Results show that the platform has been useful to inspect and modify several trajectories in clinical routine. The higher impact on cases with DSA is explained by the fact that our ROSA robot planning station version is not natively able to load and register DSA datasets.

The impact of zSpace widescreen, volume rendering, and stereo visualization which have been used for the verification of SEEG trajectories has not been quantified. Regarding visualization, the most important lesson learned is that 3D stereo can sometimes provide great insight into the surgical field, but it is a complementary view to the 2D tri-planar, which has its own strengths.

Although the Niguarda group report use of multiple tools, 3D Slicer seems one of its main development platforms. They have used it to visualize two implantation plans versions (manual versus automatic) at the same time using two sets of lines with two different colors. SYLVIUS extends the idea of visualizing different versions of a plan to keep track of the evolution of the plan on time. This feature may be used to visualize/study the adherence of the surgical plan to the epileptology draft plan and to compare the post-operative location of electrodes with the surgical plan -which can also be obtained with SEEG Assistant [26] besides other post-operative functionality-. In our opinion, 3D Slicer is a powerful general-purpose platform that allows for great control over processing, rendering, and data import, but this versatility comes with the cost of a more involved user interface. As data is untagged, tools cannot check if required inputs are present on the study to enable/disable user interaction and whenever a processing tool is used, its inputs must be manually selected by name from drop-down lists. Nevertheless, its generality might be attractive for the most technically capable clinical users. Automatic planning is also available in this system in contrast to SYLVIUS.

EpiNav provides a very interesting tool that gives the user a risk profile along the length of a selected trajectory [31], which we consider complementary to our vessel collision detection tool which looks at the same problem but in the electrode direction. The reason is EpiNav provides only a distance to risky structures, but the direction is lost. In our tool, direction is perceived, but depth is mapped to intensity which is not as precise. Although our tool uses the GPU to provide fast results, EpiNav has also employed the GPU to compute new trajectories for the user (a review of different computer-assisted planning studies for SEEG can be seen in [28]), which for us will be the subject of future work.

Regarding case construction, fixed registration schemes are described in [30] for EpiNav, where everything is registered to T1-Gd, and in [20] for the Niguarda workflow where everything is registered to DSA. Our architecture offers the possibility to apply both registration strategies, plus a variety of hybrid approaches (e.g.: case depicted in Figure 5). Choosing one dataset to be always the reference image of the registration is not optimal. For example, DSA may register better to CT, and T1-Gd to T1. Even worse, when the SYLVIUS pipeline starts, none of the above images are usually present (e.g.: T1+FreeSurfer+PET). Furthermore, our strategy based on early data annotation and relative transforms allows SYLVIUS users to completely avoid repeating the same transformation for paired data as described in steps 1.4.2.2 to 1.4.2.7 for EpiNav [30]. The example provided is for DWI tractography, which in our architecture happens automatically and transparently to the user. SYLVIUS knows that tractography shares the same space as its reference image (i.e.: b0), and places it correctly upon its registration. Avoiding this interaction can become an advantage for studies like FreeSurfer from which we currently import 107 distinct paired elements (volumes and meshes).

Another benefit of relative transformations, as in IBIS[32], is avoiding image resampling upon registration, preventing unnecessary image degradation[49]. Flat registration schemes with resampling, where everything is registered to a single image, resample N-1 datasets once. For more flexible registration schemes, the worst-case is one dataset being resampled N-1 times. In the case depicted in Figure 5, each FreeSurfer volume would have been resampled 4 times. Resampling, besides deteriorating the image[49], prevents processing (e.g.: marching cubes) to give identical results before and after registration.

As Freesurfer cannot run on Windows natively, we have provided doctors with a Linux-based Freesurfer virtual machine so that it can be processed in the same physical machine. Sharing a folder between the host and the virtual machine has shown useful to aid in data transfer.

Our design has a limitation of requiring a T1 for epileptology planning, a T1-Gd for Neurosurgery and review, and a CTpost for extracting the final position of the electrodes. This decision is based on our local workflow and we are aware that centers have distinct pipelines, for example using MR for the postoperative assessment. This can be easily changed and will be configurable in newer versions. Future work will also focus on providing a Frame and a Navigator step to substitute the Robot step in institutions that do not employ a robot for the implantation.

Beyond the initial intended goal of being a clinical tool, SYLVIUS has raised research questions arising from its ability to combine different data modalities. In Figure 18 we can see an image that contains a segmented electrode plan, filtered white matter tracts, anatomical information, and electrical readings. We expect that SYLVIUS could find utility in providing a link between the anatomical pathways estimated by the DWI and the SEEG electrical patterns which could be of interest for understanding epileptic seizure propagation, validating DWI tractography algorithms, or measure axonal propagation speed. We believe that this could be the subject of further research and that SYLVIUS and especially its dedicated DWI filtering tools based on electrode and contact positions could aid in the study of such relations.

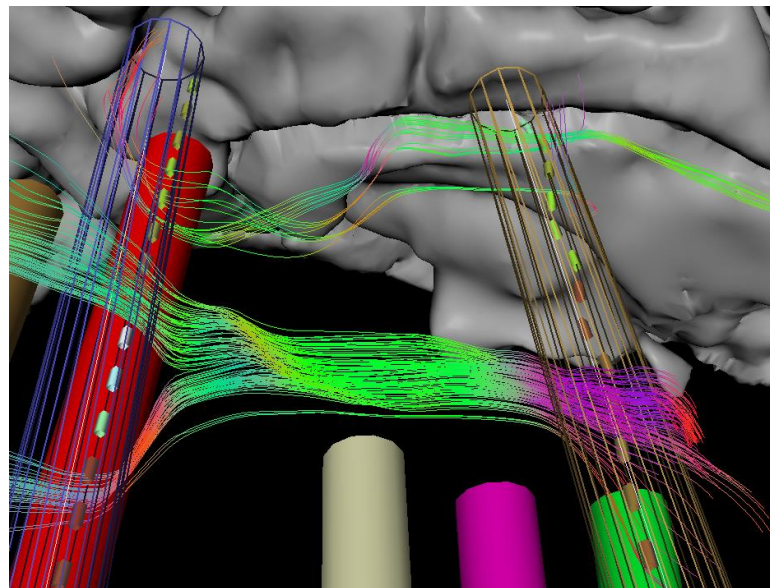


Figure 18 Tracts passing through two security zones (in wireframe), a Freesurfer segmentation (back), and electrical data from an EDF file mapped onto segmented contacts (colored cylinders)

We are currently collecting data about other stereotactic uses –DBS for anorexia nervosa and laser interstitial thermal therapy (LiTT) for tumor and epilepsy surgery - and preliminary data suggests that SYLVIUS has been useful in some steps of the procedures (i.e.: exploring DWI tracks to stimulate and vital structures to protect). We will attempt to provide customized workflows for those kinds of interventions in the future.

5. CONCLUSION

In this paper, we present SYLVIOUS, a software platform intended to facilitate and improve the complex workflow of epilepsy surgery providing pre and postoperative tools for electrode implantation and EZ resection. The software uses early data annotation and relative transformations to avoid unnecessary image resampling, automatically configure tools, and simplify the transfer of electrode plans referred to different images. Novel tools for DWI tractography in SEEG have also been described. Lastly, we provide a compact head-tracking 3D platform to visualize complex anatomical structures such as vessels or segmented white matter tracts.

ACKNOWLEDGMENTS

We would like to thank “la Caixa” Banking Foundation for supporting the project. We would also like to thank the epilepsy clinical staff of the Hospital del Mar (Barcelona, Spain) for their guidance and collaboration throughout the project.

CONFLICT OF INTEREST

Alfredo Higuera-Esteban, Ignacio Delgado-Martínez and Luis Serra are employees of Galgo Medical SL. Luis Serra is a shareholder of Galgo Medical SL.

REFERENCES

- [1] K.D. Laxer, E. Trinka, L.J. Hirsch, F. Cendes, J. Langfitt, N. Delanty, T. Resnick, S.R. Benbadis, The consequences of refractory epilepsy and its treatment, *Epilepsy Behav.* 37 (2014) 59–70. <https://doi.org/10.1016/j.yebeh.2014.05.031>.
- [2] P. Kwan, M.J. Brodie, Early Identification of Refractory Epilepsy, *N. Engl. J. Med.* 342 (2002) 314–319. <https://doi.org/10.1056/nejm200002033420503>.
- [3] L. Jehi, The epileptogenic zone: Concept and definition, *Epilepsy Curr.* 18 (2018) 12–16. <https://doi.org/10.5698/1535-7597.18.1.12>.
- [4] C. Munari, J. Bancaud, The role of stereo-EEG in the evaluation of partial epileptic seizures, *The Epilepsies*. London: Butterworths. (1985) 267–306.
- [5] J. Talairach, J. Bancaud, Lesion, "irritative" zone and epileptogenic focus, *Stereotact. Funct. Neurosurg.* 27 (1966) 91–94.
- [6] H.O. Lüders, I. Najm, D. Nair, P. Widdess-Walsh, W. Bingman, The epileptogenic zone: General principles, *Epileptic Disord.* 8 (2006) 1–9. <https://doi.org/10.3109/9780203091708-107>.
- [7] F. Rosenow, H. Lüders, Presurgical evaluation of epilepsy, *Brain.* 124 (2001) 1683–1700. <https://doi.org/10.1093/brain/124.9.1683>.
- [8] F. Cardinale, M. Rizzi, E. Vignati, M. Cossu, L. Castana, P. d'Orio, M. Revay, M. Della Costanza, L. Tassi, R. Mai, I. Sartori, L. Nobili, F. Gozzo, V. Pelliccia, V. Mariani, G. Lo Russo, S. Francione, Stereoelectroencephalography: Retrospective analysis of 742 procedures in a single centre, *Brain.* 142 (2019) 2688–2704. <https://doi.org/10.1093/brain/awz196>.
- [9] J. Gonzalez-Martinez, J. Mullin, S. Vadera, J. Bulacio, G. Hughes, S. Jones, R. Enatsu, I. Najm, Stereotactic placement of depth electrodes in medically intractable epilepsy., *J.*

- Neurosurg. 120 (2014) 639–44. <https://doi.org/10.3171/2013.11.JNS13635>.
- [10] F. Cardinale, G. Casaceli, F. Raneri, J. Miller, G. Lo Russo, Implantation of Stereoelectroencephalography Electrodes: A Systematic Review, *J. Clin. Neurophysiol.* 33 (2016) 490–502. <https://doi.org/10.1097/WNP.0000000000000249>.
 - [11] M. Nowell, R. Sparks, G. Zombori, A. Miserocchi, R. Rodionov, B. Diehl, T. Wehner, G. Baio, G. Trevisi, M. Tisdall, S. Ourselin, A.W. Mcevoy, J. Duncan, Comparison of computer-assisted planning and manual planning for depth electrode implantations in epilepsy, *J. Neurosurg.* (2015) 1–3. <https://doi.org/10.3171/2015.6.JNS15487>.
 - [12] J. Wellmer, Y. Parpaley, S. Rampp, S. Popkirov, H. Kugel, Ü. Aydin, C.H. Wolters, M. von Lehe, J. Voges, Lesion guided stereotactic radiofrequency thermocoagulation for palliative, in selected cases curative epilepsy surgery, *Epilepsy Res.* 121 (2016) 39–46. <https://doi.org/10.1016/j.eplepsyres.2016.01.005>.
 - [13] K.H. Fritzsche, P.F. Neher, I. Reicht, T. van Bruggen, C. Goch, M. Reiser, M. Nolden, S. Zelzer, H.P. Meinzer, B. Stieltjes, MITK diffusion imaging, *Methods Inf. Med.* 51 (2012) 441–448. <https://doi.org/10.3414/ME11-02-0031>.
 - [14] F. Dell'Acqua, P. Scifo, G. Rizzo, M. Catani, A. Simmons, G. Scotti, F. Fazio, A modified damped Richardson-Lucy algorithm to reduce isotropic background effects in spherical deconvolution, *Neuroimage.* 49 (2010) 1446–1458. <https://doi.org/10.1016/j.neuroimage.2009.09.033>.
 - [15] J.D. Tournier, F. Calamante, A. Connelly, MRtrix: Diffusion tractography in crossing fiber regions, *Int. J. Imaging Syst. Technol.* 22 (2012) 53–66. <https://doi.org/10.1002/ima.22005>.
 - [16] H.J. Huppertz, J. Wellmer, A.M. Staack, D.M. Altenmüller, H. Urbach, J. Kröll, Voxel-based 3D MRI analysis helps to detect subtle forms of subcortical band heterotopia, *Epilepsia.* 49 (2008) 772–785. <https://doi.org/10.1111/j.1528-1167.2007.01436.x>.
 - [17] S.M. Smith, M. Jenkinson, M.W. Woolrich, C.F. Beckmann, T.E.J. Behrens, H. Johansen-Berg, P.R. Bannister, M. De Luca, I. Drobnjak, D.E. Flitney, R.K. Niazy, J. Saunders, J. Vickers, Y. Zhang, N. De Stefano, J.M. Brady, P.M. Matthews, Advances in functional and structural MR image analysis and implementation as FSL, *Neuroimage.* 23 (2004) 208–219. <https://doi.org/10.1016/j.neuroimage.2004.07.051>.
 - [18] M.A. Jatoti, N. Kamel, A.S. Malik, I. Faye, T. Begum, A survey of methods used for source localization using EEG signals, *Biomed. Signal Process. Control.* 11 (2014) 42–52. <https://doi.org/10.1016/j.bspc.2014.01.009>.
 - [19] B. Fischl, FreeSurfer, *Neuroimage.* 62 (2012) 774–781. <https://doi.org/10.1016/j.neuroimage.2012.01.021>.
 - [20] F. Cardinale, M. Cossu, L. Castana, G. Casaceli, M.P. Schiariti, A. Miserocchi, D. Fuschillo, A. Moscato, C. Caborni, G. Arnulfo, G. Lo Russo, Stereoelectroencephalography: Surgical methodology, safety, and stereotactic application accuracy in 500 procedures, *Neurosurgery.* 72 (2013) 353–366. <https://doi.org/10.1227/NEU.0b013e31827d1161>.
 - [21] F. Cardinale, M. Rizzi, P. D'Orio, G. Casaceli, G. Arnulfo, M. Narizzano, D. Scorza, E. De Momi, M. Nichelatti, D. Redaelli, M. Sberna, A. Moscato, L. Castana, A new tool for touch-free patient registration for robot-assisted intracranial surgery: Application accuracy from a phantom study and a retrospective surgical series, *Neurosurg. Focus.* 42 (2017) 1–7. <https://doi.org/10.3171/2017.2.FOCUS16539>.
 - [22] F. Cardinale, G. Pero, L. Quilici, M. Piano, P. Colombo, A. Moscato, L. Castana, G. Casaceli, D. Fuschillo, L. Gennari, M. Cenzato, G. Lo Russo, M. Cossu, Cerebral Angiography for Multimodal Surgical Planning in Epilepsy Surgery: Description of a New Three-Dimensional Technique and Literature Review, *World Neurosurg.* 84 (2015) 358–367. <https://doi.org/10.1016/j.wneu.2015.03.028>.
 - [23] C. Caborni, E. De Momi, L. Antiga, A. Hammoud, G. Ferrigno, F. Cardinale, Automatic

- trajectory planning in Stereo-electroencephalography image guided neurosurgery, *Int. J. Comput. Assist. Radiol. Surg.* 7 (2012) S126–S127.
<https://doi.org/10.13140/2.1.4564.4806>.
- [24] E. De Momi, C. Caborni, F. Cardinale, L. Castana, G. Casaceli, M. Cossu, L. Antiga, G. Ferrigno, Automatic Trajectory Planner for StereoElectroEncephaloGraphy Procedures: A Retrospective Study, *IEEE Trans. Biomed. Eng.* 60 (2013) 986–993.
<https://doi.org/10.1109/TBME.2012.2231681>.
 - [25] D. Scorza, S. Moccia, G. De Luca, L. Plaino, F. Cardinale, L.S. Mattos, L. Kabongo, E. De Momi, Safe electrode trajectory planning in SEEG via MIP-based vessel segmentation, *Proc. SPIE 10135, Med. Imaging 2017 Image-Guided Proced. Robot. Interv. Model.* 10135 (2017) 101352C-101352C8. <https://doi.org/10.1117/12.2254474>.
 - [26] M. Narizzano, G. Arnulfo, S. Ricci, B. Toselli, M. Tisdall, A. Canessa, M.M. Fato, F. Cardinale, SEEG assistant: a 3DSlicer extension to support epilepsy surgery, *BMC Bioinformatics.* 18 (2017) 124. <https://doi.org/10.1186/s12859-017-1545-8>.
 - [27] M. Nowell, R. Sparks, G. Zombori, A. Miserocchi, R. Rodionov, B. Diehl, T. Wehner, G. Baio, G. Trevisi, M. Tisdall, S. Ourselin, A.W. McEvoy, J. Duncan, Comparison of computer-assisted planning and manual planning for depth electrode implantations in epilepsy, *J. Neurosurg.* 124 (2016) 1820–1828.
<https://doi.org/10.3171/2015.6.JNS15487>.
 - [28] V.N. Vakharia, R. Sparks, A. Miserocchi, S.B. Vos, A. O’Keeffe, R. Rodionov, A.W. McEvoy, S. Ourselin, J.S. Duncan, Computer-Assisted Planning for Stereoelectroencephalography (SEEG), *Neurotherapeutics.* 16 (2019) 1183–1197.
<https://doi.org/10.1007/s13311-019-00774-9>.
 - [29] M. Nowell, R. Rodionov, G. Zombori, R. Sparks, G. Winston, J. Kinghorn, B. Diehl, T. Wehner, A. Miserocchi, A.W. McEvoy, S. Ourselin, J. Duncan, Utility of 3D multimodality imaging in the implantation of intracranial electrodes in epilepsy, *Epilepsia.* 56 (2015) 403–413. <https://doi.org/10.1111/epi.12924>.
 - [30] M. Nowell, R. Rodionov, G. Zombori, R. Sparks, M. Rizzi, S. Ourselin, A. Miserocchi, A. McEvoy, J. Duncan, A Pipeline for 3D Multimodality Image Integration and Computer-assisted Planning in Epilepsy Surgery, *J. Vis. Exp.* (2016) 1–10.
<https://doi.org/10.3791/53450>.
 - [31] G. Zombori, R. Rodionov, M. Nowell, M.A. Zuluaga, M.J. Clarkson, C. Micallef, B. Diehl, T. Wehner, A. Miserochi, A.W. McEvoy, J.S. Duncan, S. Ourselin, A computer assisted planning system for the placement of sEEG electrodes in the treatment of epilepsy, Stoyanov D., Collins D.L., Sakuma I., Abolmaesumi P., Jannin P. *Inf. Process. Comput. Interv. IPCAI 2014. Lect. Notes Comput. Sci.* 8498 (2014) 118–127.
https://doi.org/10.1007/978-3-319-07521-1_13.
 - [32] S. Drouin, A. Kochanowska, M. Kersten-Oertel, I.J. Gerard, R. Zelmann, D. De Nigris, S. Bériault, T. Arbel, D. Sirhan, A.F. Sadikot, J.A. Hall, D.S. Sinclair, K. Petrecca, R.F. DelMaestro, D.L. Collins, IBIS: an OR ready open-source platform for image-guided neurosurgery, *Int. J. Comput. Assist. Radiol. Surg.* 12 (2017) 363–378.
<https://doi.org/10.1007/s11548-016-1478-0>.
 - [33] R. Zelmann, S. Bériault, K. Mok, C. Haegelen, J. Hall, G.B. Pike, A. Olivier, D.L. Collins, Automatic Optimization of Depth Electrode Trajectory Planning, *Clin. Image-Based Proced. Transl. Res. Med. Imaging.* 9958 (2016) 99–107. <https://doi.org/10.1007/978-3-319-46472-5>.
 - [34] S. Bériault, F. Al Subaie, D.L. Collins, A.F. Sadikot, G.B. Pike, A multi-modal approach to computer-assisted deep brain stimulation trajectory planning, *Int. J. Comput. Assist. Radiol. Surg.* 7 (2012) 687–704. <https://doi.org/10.1007/s11548-012-0768-4>.
 - [35] S. Miocinovic, A.M. Noecker, C.B. Maks, C.R. Butson, C.C. McIntyre, Cicerone: Stereotactic neurophysiological recording and deep brain stimulation electrode placement

- software system, *Acta Neurochir. Suppl.* 97 (2007) 561–567. https://doi.org/10.1007/978-3-211-33081-4_65.
- [36] P.F. D’Haese, S. Pallavaram, R. Li, M.S. Remple, C. Kao, J.S. Neimat, P.E. Konrad, B.M. Dawant, CranialVault and its CRAVE tools: A clinical computer assistance system for deep brain stimulation (DBS) therapy, *Med. Image Anal.* 16 (2012) 744–753. <https://doi.org/10.1016/j.media.2010.07.009>.
 - [37] C. Essert, C. Haegelen, P. Jannin, Automatic computation of electrodes trajectory for deep brain stimulation, *Int. Work. Med. Imaging Virtual Real.* 6326 LNCS (2010) 149–158. https://doi.org/10.1007/978-3-642-15699-1_16.
 - [38] R.A. Kockro, Y.T. Tsai, I. Ng, P. Hwang, C. Zhu, K. Agusanto, L.X. Hong, L. Serra, DEX-Ray: Augmented reality neurosurgical navigation with a handheld video probe, *Neurosurgery.* 65 (2009) 795–807. <https://doi.org/10.1227/01.NEU.0000349918.36700.1C>.
 - [39] R.A. Kockro, L. Serra, T.T. Yeo, C. Chan, Y.Y. Sitoh, G.G. Chua, E. Lee, Y.H. Lee, H. Ng, W.L. Nowinski, Planning and simulation of neurosurgery in a virtual reality environment, *Neurosurgery.* 46 (2000) 118–137. <https://doi.org/10.1093/neurosurgery/46.1.118>.
 - [40] R.R. Shamir, M. Horn, T. Blum, J. Mehrkens, Y. Shoshan, L. Joskowicz, N. Navab, Trajectory planning with augmented reality for improved risk assessment in image-guided keyhole neurosurgery, *IEEE Int. Symp. Biomed. Imaging From Nano to Macro.* (2011) 1873–1876. <https://doi.org/10.1109/ISBI.2011.5872773>.
 - [41] I. Aganj, B.T.T. Yeo, M.R. Sabuncu, B. Fischl, On removing interpolation and resampling artifacts in rigid image registration, *IEEE Trans. Image Process.* 22 (2013) 816–827. <https://doi.org/10.1109/TIP.2012.2224356>.
 - [42] R. Wang, T. Benner, A.G. Sorensen, V.J. Wedeen, Diffusion Toolkit : A Software Package for Diffusion Imaging Data Processing and Tractography, *Proc. Intl. Soc. Mag. Reson. Med.* 15 (2007) 3720.
 - [43] D. Stein, K.H. Fritzsche, M. Nolden, H.P. Meinzer, I. Wolf, The extensible open-source rigid and affine image registration module of the Medical Imaging Interaction Toolkit (MITK), *Comput. Methods Programs Biomed.* 100 (2010) 79–86. <https://doi.org/10.1016/j.cmpb.2010.02.008>.
 - [44] A. Higuera-Esteban, I. Delgado-Martínez, L. Serrano, G. Conesa, M.A. González Ballester, L. Serra, Volume rendering depth mapping for fast vessel identification during intracranial deep electrode planning, *Int. J. Comput. Assist. Radiol. Surg. (Suppl 1).* 14 (2019) 150–151. <https://doi.org/10.1007/s11548-019-01969-3>.
 - [45] G. Arnulfo, M. Narizzano, F. Cardinale, M.M. Fato, J.M. Palva, Automatic segmentation of deep intracerebral electrodes in computed tomography scans., *BMC Bioinformatics.* 16 (2015) 12–99. <https://doi.org/10.1186/s12859-015-0511-6>.
 - [46] S. Medina Villalon, R. Paz, N. Roehri, S. Lagarde, F. Pizzo, B. Colombet, F. Bartolomei, R. Carron, C.G. Bénar, EpiTools, A software suite for presurgical brain mapping in epilepsy: Intracerebral EEG, *J. Neurosci. Methods.* 303 (2018) 7–15. <https://doi.org/10.1016/j.jneumeth.2018.03.018>.
 - [47] A. Higuera-Esteban, J. Ojeda, I. Delgado-Martínez, C.P. Enríquez, L. Serrano, A. Principe, M.A. González Ballester, R. Rocamora, L. Serra, G. Conesa, Automatic segmentation of deep brain electrodes used in stereotactic electroencephalography (SEEG), *Int. J. Comput. Assist. Radiol. Surg.* 13 (2018) 79–80. <https://doi.org/10.1007/s11548-018-1766-y>.
 - [48] A. Higuera-Esteban, I. Delgado-Martínez, L. Serrano, A. Principe, M.A. González Ballester, R. Rocamora, L. Serra, G. Conesa, Diffusion Weighted Imaging (DWI) tractography filtering tools for Stereotactic Electro-Encephalography (SEEG), 2020. <https://doi.org/10.1007/s11548-020-02171-6>.

- [49] A. Li, K. Mueller, T. Ernst, Methods for efficient, high quality volume resampling in the frequency domain, IEEE Vis. 2004 - Proceedings, VIS 2004. (2004) 3–10.
<https://doi.org/10.1109/visual.2004.70>.